CHIN. PHYS. LETT. Vol. 31, No. 7 (2014) 074301

# Photoacoustic Imaging of Animals with an Annular Transducer Array *

YANG Di-Wu(杨迪武)[1**], ZHOU Zhi-Bin(周智彬)[1], ZENG Lv-Ming(曾吕明)[2], ZHOU Xin(周昕)[1], CHEN Xing-Hui(陈星辉)[1]

[1]*Department of Physics and Engineering, Hunan University of Technology, Zhuzhou 412000*
[2]*Key Lab of Optic-Electronic and Communication, Jiangxi Sciences and Technology Normal College, Nanchang 330038*

(Received 1 April 2014)

*A photoacoustic system with an annular transducer array is presented for rapid, high-resolution photoacoustic tomography of animals. An eight-channel data acquisition system is applied to capture the photoacoustic signals by using multiplexing and the total time of data acquisition and transferring is within 3 s. A limited-view filtered back projection algorithm is used to reconstruct the photoacoustic images. Experiments are performed on a mouse head and a rabbit head and clear photoacoustic images are obtained. The experimental results demonstrate that this imaging system holds the potential for imaging the human brain.*

*PACS:* 43.35.+d, 87.57.C− 43.60.+d, 43.80.+p DOI: 10.1088/0256-307X/31/7/074301

Photoacoustic imaging (PAI) is a novel noninvasive imaging modality based on the photoacoustic effect.[1−7] In principle, when irradiated by a short-pulsed laser beam, tissue absorbs the light and generates a pressure rise by thermo-elastic expansion. By detecting the acoustic pressure instead of photons, PAI can reach several-centimeters of penetration depth in tissue, while maintaining better optical absorption contrast and high ultrasonic resolution. Now PAI has been extensively studied in various biological applications.[8−16]

Brain imaging can facilitate the understanding of neural activities and cognitive phenomena. The current modalities employed for brain imaging include magnetic resonance imaging (MRI), ultrasonography, and optical imaging. MRI is the most widespread approach in the field of functional brain mapping while it is costly and provides weak functional signals.[17] Ultrasonography is commonly used for pediatric brain imaging, while it is limited by the low acoustic impedance of soft brain tissues.[18] Optical imaging in brain imaging suffers from its inherently low spatial resolution.[19] Photoacoustic imaging combines the advantages of pure optical imaging and pure ultrasonic imaging[20] and holds the potential for human brain imaging.

Wang *et al.* developed a ring-ultrasound-array photoacoustic tomography system for small animal imaging using a 64-channel acquisition system,[21] and Xing *et al.* applied a full-field 3D photoacoustic imaging system based on a plane transducer array with a paralleled acquisition system.[22] Wang *et al.* successfully applied the photoacoustic method for imaging a monkey skull and a human skull.[23−25] Their experimental results can demonstrate that light can penetrate thick skull and the produced (PA) signals are sufficiently detectable. However, the imaging system with a single transducer point-to-point scanning required a long time for collecting the PA signals, which hinders the clinical applications.

In this Letter, we present a photoacoustic imaging system based on an annular transducer array for imaging big animals. The system is based on a 256-element annular ultrasonic transducer array with 50-mm radius of curvature, which is suitable for imaging big animals. An eight-channel acquisition system is used to capture the photoacoustic signals controlled by channel detection electronics, and the total time of data acquisition and transferring is within 3 s. A filtered back projection algorithm with deconvolution is used to reconstruct the photoacoustic images. Experiments were performed on a mouse brain and a rabbit brain, and clearly photoacoustic images are obtained. The experimental results demonstrate that this PA imaging system has the ability to quickly and conveniently image a big animal and holds the potential solution for imaging the human brain.

When an annular transducer array is used to detect laser-induced photoacoustic signals, due to the finite bandwidth and size of the individual transducer of the transducer array, the impulse response of the transducer must be taken into account. Images were reconstructed by using a filtered back-projection algorithm with deconvolution.[26] The deconvolution is performed in the frequency by using the fast Fourier transform (FFT)[27]

$$\iint_{|r|=ct} A(r)ds = \frac{4\pi C_p kt}{\beta r_p}\left(\frac{P'(\omega)W(\omega)}{P'_o(\omega)}\right),$$

*Supported by the National Natural Science Foundation of China under Grant Nos 11304129 and 11374094, the Hunan-Provincial Natural Science Foundation under Grant No 14JJ3122, the Science and Technology Pillar Program of Jiangxi Province under Grant No 2009BSA12700, and the Natural Science Foundation of Hunan University of Technology under Grant No 2011HZX16.

**Corresponding author. Email: yangdiwu@163.com

© 2014 Chinese Physical Society and IOP Publishing Ltd

where $\beta$ is the isobaric volume expansion coefficient, $C_p$ is the specific heat, $P'(\omega)$ and $P'_o(\omega)$ are the Fourier transforms of recorded PA signals from the sample and the recorded PA signal from the point source, respectively, $W(\omega)$ is a window function used to band-limit the signals and to taper the high-frequency components smoothly to zero.[28]

Figure 1 depicts the block diagram of the annular array photoacoustic system. A Ti sapphire (Symphotics TII, LS-2134) laser optically pumped with a Q-switched Nd:YAG laser delivers 8–12 ns pulses at 15 Hz with the wavelength of 1064 nm, providing laser pulses to irradiate the sample for generating the photoacoustic signals. The laser beam is positioned at the center of the transducer, homogenized by a circular profile diffuser and strikes the stage orthogonal to the imaging plane of the transducer for maximum uniformity. The transducer array consists of 256 elements arranged along a 300-deg arc with a 50-mm radius of curvature. The array was designed as building block for a 308-element closed-ring system. The array was custom fabricated by Doppler Electronic Technologies (Guangzhou, China) by using piezocomposite technology for high sensitivity and signal-noise-ratio (SNR). The central frequency of the array is 7.5 MHz and the bandwidth is beyond 75%. The individual element of the array features an elevation height of 8 mm, an elementary pitch of 1.1 mm and an element inter space of 0.04 mm, and the relative pulse-echo sensitivity is −29 dB. The lateral resolution of the imaging system is about 0.1 mm at the center of the transducer array[11] and the radial resolution is a nearly constant value of 0.08 mm throughout the imaging area.

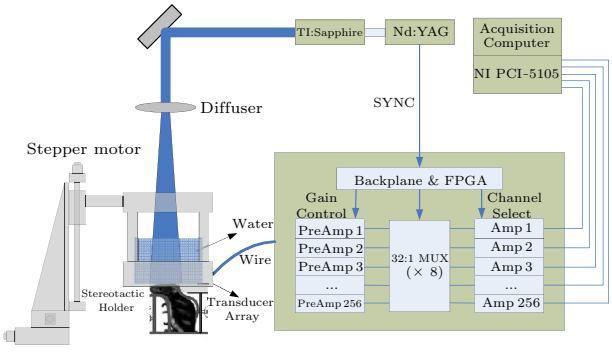


**Fig. 1.** Block diagram of the annular array photoacoustic system. Definitions: FPGA=field programmable gate array; MUX=multiplexer.

The bottom of the annular array was sealed with an elastic transparent membrane and the side face was sealed up with polyethylene materials to form a water tank. A thin layer of ultrasonic coupling gel was applied to couple the sample and the membrane. The transducer array was mounted on a stepper motor to adjust the position up and down. By multiplexing, the produced photoacoustic signals were captured by an eight-channel acquisition card (NI PCI5105, American). The card features a high-speed 12-bit analogue-to-digital converter with a sampling rate of 60 MHz. Due to the multiplexing, 32 laser firings were required to generate a single 256-channel capture. The total time of data acquisition and transferring is within 3 s. After 256 series, signals were transferred to the computer for further data processing by using MATLAB (version 8.0, Mathworks, USA), images were reconstructed with the limited-field filtered back projection (LFBP) algorithm. In the experiments, the ultrasound velocity is assumed to be 1500 m/s for photoacoustic reconstruction.

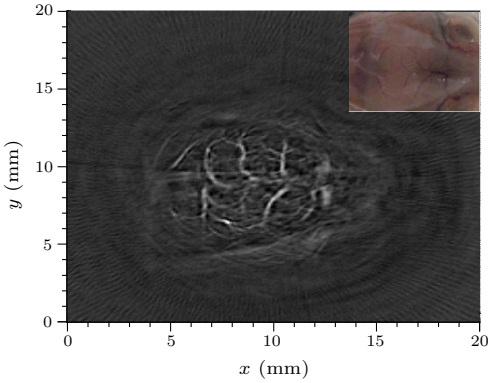


**Fig. 2.** The PA imaging of the superficial layer of a mouse brain acquired with the skin and skull intact. The inset is the photograph of the mouse brain surface after the experiment.

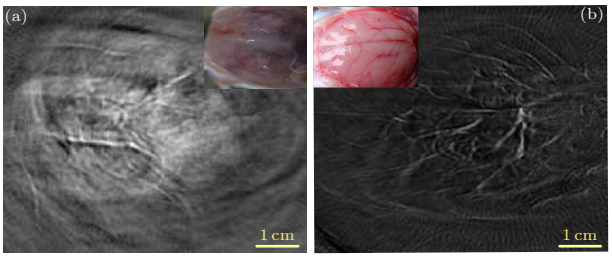


**Fig. 3.** The PA imaging of a rabbit brain. (a) A PA image of the skull of the rabbit, and the inset is a photograph of the rabbit brain with the skull intact. (b) PA imaging of brain cortical vasculature of the rabbit with the skull intact, where the inset is the open-skull photograph of the rabbit brain after experiments.

To test the PA imaging system with the capacity of imaging of the anatomical structure of the brain, the first experiment was performed on a mouse brain. Before the experiment, the fur on the skull of the mouse was shaven and chemically depilated. Before PA imaging, a dose of 40 mg/kg sodium pentobarbital was administrated to anesthetize the mouse. A custom-built stereotaxic holder was used to keep the mouse immobilized. Figure 2 shows the photoacoustic image of the vascular distribution in the mouse brain. The inset is the open-skull photograph of the mouse brain surface after the experiment. A satisfactory match between

the photograph and the reconstructed image can be seen such that the main vessels and the vascular ramifications in the mouse brain can be imaged clearly and accurately, in addition to the top surfaces of the eyes.

To verify that this PA imaging has the ability of imaging big animal, a second experiment was performed. A female New Zealand white rabbit, 6–8 weeks of age, was used. Before the experiment, the rabbit was sacrificed by using a lethal injection of Beuthansia (150 mg/kg, intravenous). Then the fur and skin on the rabbit brain were carefully removed and the skull was retained intact. Figure 3 is the PA imaging of the rabbit brain. Figure 3(a) is the PA image of the skull of the rabbit, and the inset is a photograph of the rabbit brain with the skull intact. Figure 3(b) is the PA imaging of brain cortical vasculature of the rabbit with the skull intact, and the inserted is an open-skull photograph of the rabbit brain after experiments. As we can see that the image is slightly distorted because of the mismatch of the speed of sound between water and skull, which may be improved by using the advanced reconstruction algorithm.[29] The experimental results demonstrate that 1064 nm light can penetrate the thick rabbit skull and the produced PA signals can be detectable by the PA imaging system.

The imaging results demonstrate that our PA imaging system has the capability of imaging not only small animals but also large animals with high sensitivity and resolution. Due to the limitation of experimental funds, an eight-channel acquisition system was used to capture the photoacoustic signals and the total time for data acquisition was within 3 s. If the 128- or 256-channel parallel acquisition system is applied, real time PA imaging will be achieved. Then we can easily trace and monitor the dynamic change in regions of interest within brain. The skull of an adult human is much thicker than that of the rabbit, while the skull of the newborn is thinner than that of an adult human. Combining the near infrared light with the corresponding optical contrast enhanced agent, such as indocyanine green and nanoshells, it will make PA imaging promising for cerebral injury detection of the newborn.

In summary, we have presented our PA imaging system with an annular transducer array for imaging brains of animals and obtain clear PA images with high optical contrast and spatial resolution. The experimental results demonstrate that our PA imaging system has the capability of imaging big animals, which holds the potential for the cerebral injury detection of the newborn. We hope that our research results can accelerate the application of PA imaging to the human brain.

## References


[1] Hoelen C G A, Mul de F F M, Pongers R and Dekker A 1998 *Opt. Lett.* **23** 648
[2] Wang X, Pang Y, Ku G, Xie X, Stoica G and Wang L V 2003 *Nat. Biotechnol.* **21** 803
[3] Yin B Z, Xing D, Wang Y, Zeng Y G, Tan Y and Chen Q 2004 *Phys. Med. Biol.* **49** 1339
[4] Yang D W, Xing D, Gu H M, Tan Y and Zeng L M 2005 *Appl. Phys. Lett.* **87** 194101
[5] Yang D W, Xing D, Tan Y, Gu H M and Yang S H 2006 *Appl. Phys. Lett.* **88** 174101
[6] Yang D W, Xing D, Yang S H and Xiang L Z 2007 *Opt. Express* **15** 15566
[7] Zeng L M, Xing D, Gu H M, Yang D W, Yang S H and Xiang L Z 2007 *Med. Phys.* **34** 556
[8] Razansky D, Vinegoni C and Ntziachristos V 2007 *Opt. Lett.* **32** 2891
[9] Zeng L M, Liu G D, Yang D W and Ji X R 2012 *Opt. Express* **20** 1237
[10] Zeng L M, Liu G D, Yang D W and Ji X R 2013 *Appl. Phys. Lett.* **102** 053704
[11] Yang D W, Zeng L M, Pan Ch N, Zhao X H and Ji X R 2013 *Opt. Express* **21** 984
[12] Cox B, Laufer J G, Arridge S R and Beard P C 2012 *J. Biomed. Opt.* **17** 061202
[13] Cai X, Li W, Kim C H, Yuan Y, Wang L H and Xia Y 2011 *ACS Nano* **5** 9658
[14] Tan Z L, Tang Z L, Wu Y B, LiaoY F, Dong W and Guo L N 2011 *Opt. Express* **19** 2426
[15] Zhang Y, Cai X, Yao J, Xing W, Wang L H and Xia Y 2014 *Angew. Chem. Int. Ed.* **53** 184
[16] Yao J, Wang L, Li C, Zhang C and Wang L V 2014 *Phys. Rev. Lett.* **112** 014302
[17] Xing W, Wang L, Maslov K I and Wang L V 2013 *Opt. Lett.* **38** 52
[18] Biswal B B, Mennes M, Zuo X N, Gohel S and Kelly C 2010 *Proc. Natl Acad. Sci.* **107** 4734
[19] Boas D A, Dale A M and Franceschini M A 2004 *Neuroimaging* **23** S275
[20] Smith S W, Chu K,. Idriss S F, N Ivancevich M, Light E D and Wolf P D 2004 *Ultrasound Med. Biol.* **30** 1365
[21] Gamelin J, Maurudis A, Aguirre A, Huang F, Guo P, Wang L H and Zhu Q 2009 *Opt. Express* **17** 10489
[22] Zhou Q, Ji X R and Xing D 2011 *Med. Phys.* **38** 1561
[23] Wang L H and Hu S 2012 *Science* **335** 1458
[24] Nie L, Guo Z and Wang L H 2011 *J. Biomed. Opt.* **16** 076005
[25] Nie L, Cai X, Maslov K, Garcia-Uribe A, Anastasio M A and Wang L H 2012 *J. Biomed. Opt. Lett.* **17** 110506
[26] Yang X and Wang L V 2008 *J. Biomed. Opt. Lett.* **13** 044009
[27] Wang Y, Xing D, Zeng Y G and Chen Q 2004 *Phys. Med. Biol.* **49** 3117
[28] Gonzates R, Woods R and Eddins S 2003 *Digital Image Processing Using MATLAB* (Upper Saddle River, New Jersey: Prentice Hall)
[29] Kruger R A, Reinecke D and Kruger G 1999 *Med. Phys.* **26** 1832